APPLIED ELEMENT METHOD IN THE SOLUTION OF PLANE PROBLEMS IN THE THEORY OF CREEP

A.S. Chepurnenko[*], A.A. Savchenko, V.S. Chepurnenko

Don State Technical University, Sotcialisticheskaya st., 162, Rostov-on-Don, 344022, Russia

*e-mail: anton_chepurnenk@mail.ru

Abstract. The article deals with the consideration of creep in the solution of plane problems by the applied element method. The derivation of the resolving equations is given, as well as the solution of the test problem for the cantilever beam. For calculations, the authors developed a program in the Matlab software package.
Keywords: creep theory, numerical methods, stress-strain state, applied element method, plane problem

1. Introduction

Applied element method (AEM) is a numerical analysis technique designed to solve the problems of mechanics of a deformable solid. Studies on this method began in 1995 at the University of Tokyo, and the name AEM was first used in [1]. The verification of the method for two-dimensional elastic problems was also performed in [1]. In [2], the problems of crack initiation and propagation were investigated, and in [3] geometrically nonlinear problems were considered. In [4], the possibility of using the method in problems of nonlinear dynamics was shown. The recent publications dedicated to AEM include [5-11].These publications deal with dynamic tasks, including seismic effects [6], demolition [7], blast loads [8], progressive collapse [5,9,10], cyclic effects [11]. The use of AEM in problems of the theory of creep has not previously been considered.

The essence of the method consists in representing the structure as a set of rigid elements of small dimensions connected by normal and shear springs corresponding respectively to the transmission of normal and tangential stresses between the elements (Fig. 1). Modeling of objects in AEM is similar to finite element modeling. At the same time, the method has a relationship with the method of discrete elements.

The material properties are set by assigning the corresponding rigidity to the springs. The stiffness of normal and shear springs is determined by the formulas:

$$K_n = \frac{E \cdot d \cdot T}{a}; \quad K_s = \frac{G \cdot d \cdot T}{a}, \tag{1}$$

where d is the distance between the springs, T is the thickness of the element, a is the length of the region represented by the spring, E and G are respectively the modulus of elasticity and the shear modulus of the material.

Compared with the finite element method (FEM), AEM has a number of significant advantages. First advantage is the simplicity of the mesh generation. When linking large and small elements, no transition elements are required (Fig. 2). In addition, the use of AEM allows to consume significantly less RAM. One rectangular element of a planar problem in AEM has 3 degrees of freedom, and in FEM it has 2 or 3 degrees of freedom at each node, that is, total 8 or 12 degrees of freedom per element. The AEM method also quite simply

allows to simulate the development of cracks by successive removal of springs on the sides of the element.
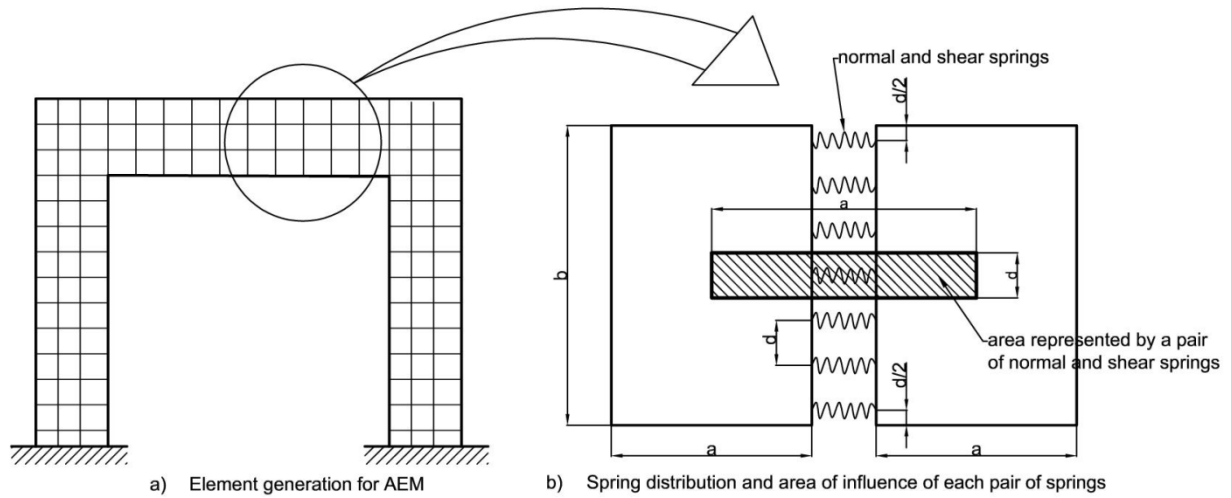

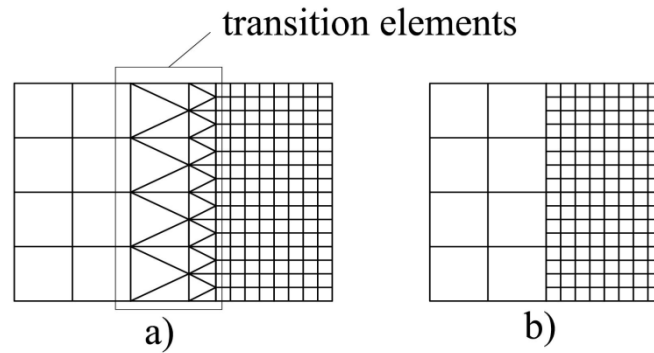**Fig. 1.** Modeling of structure in AEM

Fig. 2. Mesh generation in FEM (a) and AEM (b)

The article [5] shows the advantage of the AEM method compared to FEM in problems of progressive collapse. FEM is able to predict the structural response of small scale models well, but fails to achieve realistic collapsed shapes in case of the large structure, whereas the AEM shows convincing results in all cases.

2. Derivation of resolving equations

We consider the problem of creep calculation in solving two-dimensional problems by the AEM method. We assume that the normal and shear spring are connected to the viscous elements, then the total deformations are represented as the sum of elastic deformations and creep strains:

$$\varepsilon = \frac{\sigma}{E} + \varepsilon^*; \quad \gamma = \frac{\tau}{G} + \gamma^*. \tag{2}$$

Let the elements 1 and 2 have displacements u_1, v_1, φ_1 and u_2, v_2, φ_2 (Fig. 3). Then the deformations of the normal and shear springs will be written as:

$$\varepsilon = \frac{u_2 - u_1}{a}\cos\varphi + \frac{v_2 - v_1}{a}\sin\varphi - \frac{L(\varphi_2 - \varphi_1)\cos\alpha}{a};$$

$$\gamma = \frac{v_2 - v_1}{a}\cos\varphi - \frac{u_2 - u_1}{a}\sin\varphi - \frac{L(\varphi_2 + \varphi_1)\sin\alpha}{a}. \tag{3}$$
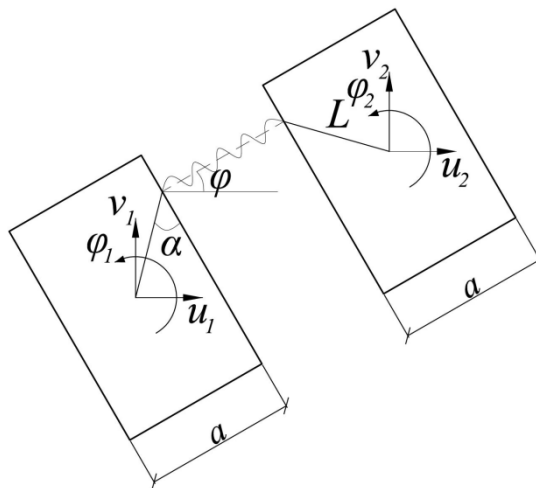
Fig. 3. To the construction of the stiffness matrix of an arbitrarily oriented spring

Relations (3) can be represented in matrix form:

$$\varepsilon = \frac{1}{a}[-\cos\varphi \quad -\sin\varphi \quad L\cos\alpha \quad \cos\varphi \quad \sin\varphi \quad -L\cos\alpha]\{U\} = \frac{1}{a}[B_n]\{U\};$$

$$\gamma = \frac{1}{a}[\sin\varphi \quad -\cos\varphi \quad -L\sin\alpha \quad -\sin\varphi \quad \cos\varphi \quad -L\sin\alpha]\{U\} = \frac{1}{a}[B_s]\{U\},$$
(4)

where $\{U\} = \{u_1 \quad v_1 \quad \varphi_1 \quad u_2 \quad v_2 \quad \varphi_2\}^T$.

The potential energy of deformation of one pair consisting of a normal and a shear spring is written as:

$$W = \frac{1}{2}d\cdot T\cdot a(\sigma\varepsilon^{el} + \tau\gamma^{el}) = \frac{1}{2}d\cdot T\cdot a[E(\varepsilon-\varepsilon^*)^2 + G(\gamma-\gamma^*)^2].$$
(5)

The indices "el" in the formula (5) correspond to elastic deformations.

Substituting (4) into (5), we obtain:

$$W = \frac{1}{2}\{U\}^T\left(K_n[B_n]^T[B_n] + K_s[B_s]^T[B_s]\right)\{U\} - \{U\}^T d\cdot T(E[B_n]^T\varepsilon^* + G[B_s]^T\gamma^*) +$$

$$+\frac{Aa}{2}\left(E\left(\varepsilon^*\right)^2 + G(\gamma^*)^2\right).$$
(6)

Minimizing the Lagrange functional $\Lambda = W - A$, where $A = \{U\}^T\{F\}$ – potential of external forces, by the displacement vector $\{U\}$ we obtain a system of linear algebraic equations:

$$[K]\{U\} = \{F\} + \{F^*\},$$
(7)

where $[K]$ – stiffness matrix, $\{F\}$ – the vector of external forces (applied in contrast to the FEM not to the nodes, but to the centers of rigid elements), $\{F^*\}$ – contribution of creep strains to the load vector.

$$[K] = K_n[B_n]^T[B_n] + K_s[B_s]^T[B_s]; \quad \{F^*\} = d\cdot T(E[B_n]^T\varepsilon^* + G[B_s]^T\gamma^*).$$
(8)

The matrix $[K]$ and the vector $\{F^*\}$ in formula (8) are written for one pair of springs. To obtain the stiffness matrix of the entire structure and the global load vector, summation over all springs is performed. The summation procedure has a similarity to the FEM, but the springs act as the finite elements, and the rigid elements themselves act as nodes.

3. Solution of test problem

The test task for a cantilever PVC polymer beam was solved, with a concentrated force F applied to the free end (Fig. 4). The initial data for the calculation was: $F = 0.2$ kN, $E = 1480$ MPa, beam length $l = 1$ m, cross-sectional height $h = 0.1$ m, section width $T = 0.05$ m. As the creep law, the Maxwell-Gurevich nonlinear equation was used in the form:

$$\frac{\partial \varepsilon^*}{\partial t} = \frac{\sigma - E_\infty \varepsilon^*}{\eta_0^*} \exp\left(\frac{\left|\sigma - E_\infty \varepsilon^*\right|}{m^*}\right), \quad \frac{\partial \gamma^*}{\partial t} = \frac{1}{2}\frac{3\tau - E_\infty \gamma^*}{\eta_0^*} \exp\left(\frac{1}{2}\frac{\left|3\tau - E_\infty \gamma^*\right|}{m^*}\right), \tag{9}$$

where m^* – velocity module, E_∞ – modulus of viscoelasticity, η_0^* – initial relaxation viscosity.
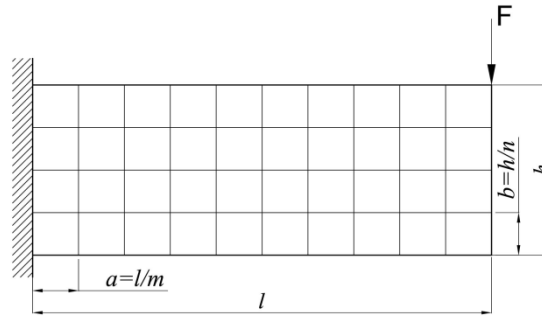

Fig. 4. Calculation scheme

Rheological parameters of PVC [12]: $E_\infty = 5990$ MPa, $\eta_0^* = 5.42 \cdot 10^7$ MPa·s, $m^* = 12.6$ MPa. The calculation was carried out step-by-step, at the first step an elastic problem was solved, then the rates of creep strains were calculated from stresses, and creep deformations at the time $t + \Delta t$ were determined using the Euler method:

$$\varepsilon_{t+\Delta t}^* = \varepsilon_t^* + \frac{\partial \varepsilon^*}{\partial t}\Delta t. \tag{10}$$

To solve the problem, the authors developed a program in the Matlab package. Figure 5 shows the curves of the maximum deflection growth for various values of m, n, p, where m is a number of segments along the length of the beam, n is a number of segments along the height of the beam and p is the number of springs on the side of the element.

It can be seen from Fig. 5 that if there is a large number of elements along the height of the beam, one spring on the side of the element is enough. In the case of only one row of elements for beam height, with a large number of springs, a satisfactory result is also obtained.

Without taking into account the shear deformations, the deflection at the end of the console at $t = 0$ can be determined from the well-known formula:

$$f = Fl^3 / (3EI), \tag{11}$$

where $I = Th^3 / 12$ – moment of inertia of the cross section.

For a material obeying the Maxwell-Gurevich equation, a solution at the end of the creep process can be obtained by replacing the instantaneous elastic modulus E in formula (11) with a long modulus $H = EE_\infty / (E + E_\infty)$. The substitution of the instantaneous and long modulus of elasticity in formula (11) gives values of 10.8 and 13.5 mm, respectively. Based on the results of numerical calculation, the values of 11 mm and 13.7 mm were obtained at $m = n = p = 20$. The indicated values turned out to be higher than the analytical values, since the shear deformation is taken into account in solving the problem in a two-dimensional formulation.

Also, the presented problem was solved in Matlab by the finite element method using rectangular finite elements. A comparison of results obtained with AEM and FEM is shown in Fig. 6. From this graph it can be seen that using FEM requires a much finer finite element mesh. The results obtained on the basis of AEM with m = 8, n = 1, p = 20, coincide with the solution using FEM with m = 150, n = 15. With a coarser grid, the FEM gives underestimated values of the deflection.
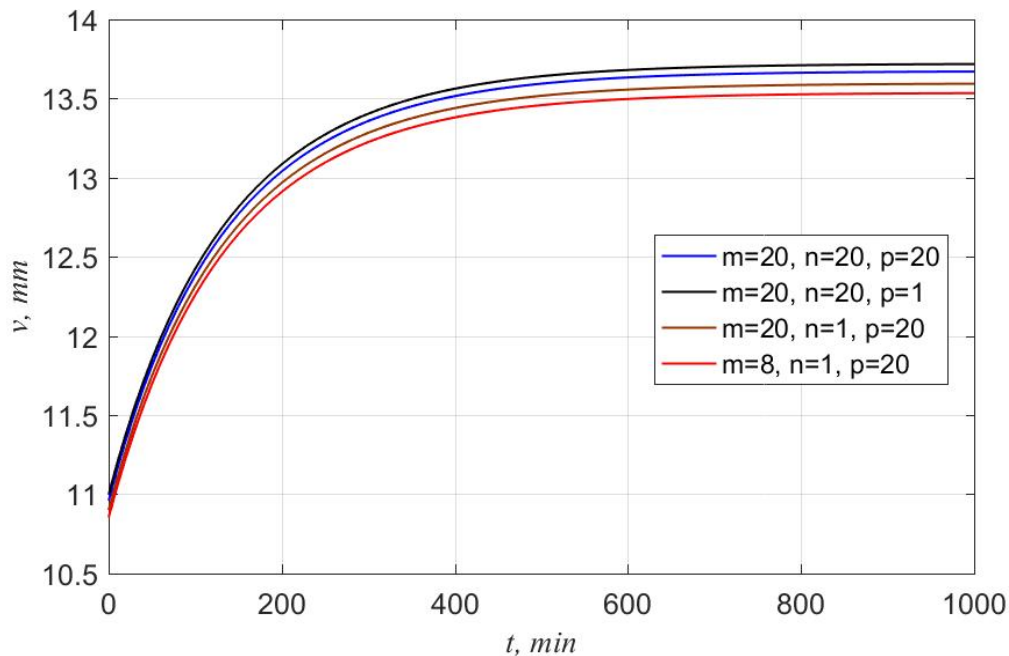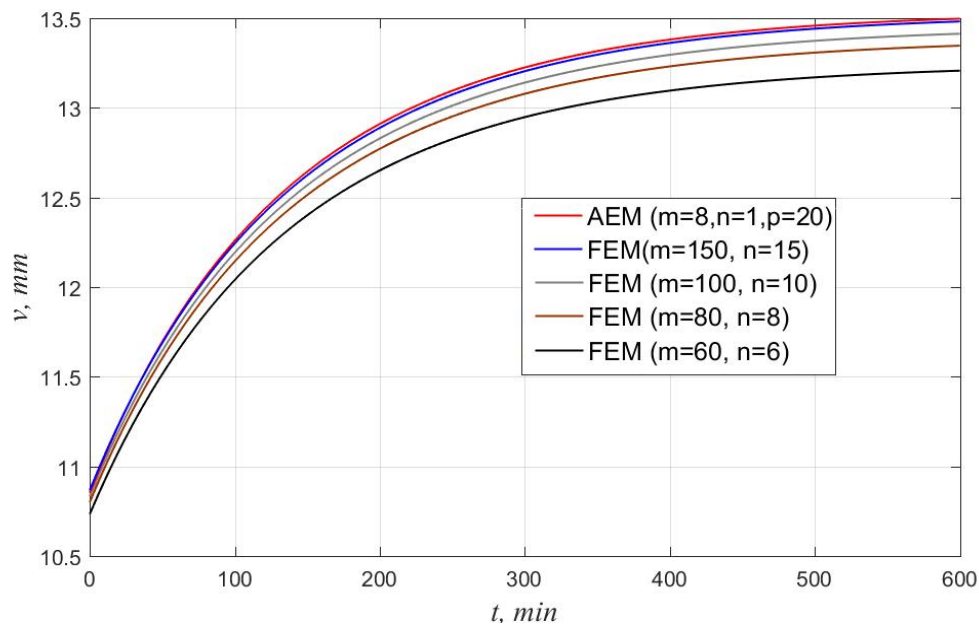
Fig. 5. Curves of the deflection growth

Fig. 6. Comparison of the results obtained with FEM and AEM

4. Conclusions

The presented example of calculation shows the possibility of applying the method in problems of creep theory. It should be noted that the proposed formulation does not take into account transverse deformations (the Poisson's ratio is equal to zero). In such problems as beams and frames bending, the influence of the Poisson's ratio can be neglected. It is also

known that the stress distribution in a homogeneous body in the case of the plane problem of the theory of elasticity is determined by a biharmonic equation for stress function that does not include the Poisson coefficient. Therefore, if only static boundary conditions are specified on the body surface, the stress distribution will not depend on the Poisson's ratio. In some cases the Poisson's ratio can have a significant effect on the stress-strain state. There is an approach that allows to take into account the Poisson's ratio, which consists in modifying the rigidity matrix [1]. This approach can also be applied in creep problems. We considered only rectangular elements, but there is a modification of the method based on the Voronoi diagram [13], where polygonal elements are used.

References
[1] Meguro K, Tagel-Din H. Applied element method for structural analysis: Theory and application for linear materials. *Structural engineering/earthquake engineering. Japan: Japan Society of Civil Engineers(JSCE).* 2000;17(1): 21-35.
[2] Tagel-Din H, Meguro K. Applied Element Simulation of RC Structures under Cyclic Loading. *Journal of Structural Engineering. Japan: ASCE.* 2001;127(11): 137-148.
[3] Tagel-Din H, Meguro K. AEM Used for Large Displacement Structure Analysis. *Journal of Natural Disaster Science. Japan.* 2002;24(1): 25-34.
[4] Tagel-Din H, Meguro K. Dynamic Modeling of Dip-Slip Faults for Studying Ground Surface Deformation Using Applied Element Method. In: *Proceedings of the 13th World Conference on Earthquake Engineering. August 1-6, 2004, Vancouver, Canada.* 2004. p.28-35.
[5] Grunwald C, Khalil AA, Schaufelberger B, Ricciardi EM, Pellecchia C, De Iuliis E, Riedel W. Reliability of collapse simulation–Comparing finite and applied element method at different levels. *Engineering Structures.* 2018;176: 265-278.
[6] Zerin A, Hosoda A, Salem H, Amanat K. Seismic performance evaluation of masonry infilled reinforced concrete buildings utilizing verified masonry properties in applied element method. *Journal of Advanced Concrete Technology.* 2017;15(6): 227-243.
[7] Simion A, Dragomir CS. The Simulation of an Industrial Building Demolition. National Institute for Research and Development in Construction. *Urbanism. Architecture. Constructions.* 2013;4(2): 67-74.
[8] Keys RA, Clubley SK. Establishing a predictive method for blast induced masonry debris distribution using experimental and numerical methods. *Engineering Failure Analysis.* 2017;82: 82-91.
[9] Michel C, Karbassi A, Lestuzzi P. Evaluation of the seismic retrofitting of an unreinforced masonry building using numerical modeling and ambient vibration measurements. *Engineering Structures.* 2018;158: 124-135.
[10] Adam JM, Parisi F, Sagaseta J, Lu X. Research and practice on progressive collapse and robustness of building structures in the 21st century. *Engineering Structures.* 2018;173: 122-149.
[11] Malomo D, Pinho R, Penna A. Using the applied element method to simulate the dynamic response of full-scale URM houses tested to collapse or near-collapse conditions. *Earthquake Engineering and Structural Dynamics.* 2018;47: 1610-1630.
[12] Dudnik AE, Chepurnenko AS, Litvinov SV. Determining the rheological parameters of polyvinylchloride, with change in temperature taken into account. *International Polymer Science and Technology.* 2017;44(1): 30-33.
[13] Worakanchana K, Meguro K. Voronoi Applied Element Method For Structural Analysis: Theory And Application For Linear And Non-Linear Materials. In: *Proceedings of the 14th World Conference on Earthquake Engineering (WCEE). October 12-17, 2008, Beijing, China.* 2008. p.12-17.